Neuronal Synchrony during Anesthesia: A Thalamocortical Model

Jane H. Sheeba, Aneta Stefanovska, and Peter V. E. McClintock
Department of Physics, Lancaster University, Lancaster LA1 4YB, United Kingdom

ABSTRACT There is growing evidence in favor of the temporal-coding hypothesis that temporal correlation of neuronal discharges may serve to bind distributed neuronal activity into unique representations and, in particular, that θ (3.5–7.5 Hz) and δ (0.5 $<$ 3.5 Hz) oscillations facilitate information coding. The θ- and δ-rhythms are shown to be involved in various sleep stages, and during anesthesia, they undergo changes with the depth of anesthesia. We introduce a thalamocortical model of interacting neuronal ensembles to describe phase relationships between θ- and δ-oscillations, especially during deep and light anesthesia. Asymmetric and long-range interactions among the thalamocortical neuronal oscillators are taken into account. The model results are compared with experimental observations. The δ- and θ-activities are found to be separately generated and are governed by the thalamus and cortex, respectively. Changes in the degree of intraensemble and interensemble synchrony imply that the neuronal ensembles inhibit information coding during deep anesthesia and facilitate it during light anesthesia.

INTRODUCTION

Neuronal communication and synchronization are crucially important features of the cooperative interaction among neuronal ensembles, endowing the brain with the marvelous capability known as cognition. The timescales of human motor and cognitive events are comparable to those of the electroencephalographic (EEG) field dynamics arising from synchronous activity, observable from within or outside the brain (1). Since EEG signals correspond to the averaged activity of large cell populations, their fluctuations can support cognitive activity only if they are sufficiently synchronized: effective communication of neuronal ensembles can be achieved only if they are oscillating in a synchronized manner. Such behavior tags those neurons to represent particular cognitive tasks, e.g., in relation to a perceptual object (2).

In this article, we present a model of interacting thalamocortical neuronal ensembles in an attempt to account for the behavior of δ- and θ-waves during anesthesia. Our model is motivated by an attempt to tackle the problem of anesthetic awareness, to provide the basic understanding needed to prevent people from inadvertently awakening during surgery. We therefore focus on ways to identify and characterize the states of deep and light anesthesia. Our starting point model is the experimental observation that both the cardiorespiratory and respiratory δ-interactions change with the depth of anesthesia in rats (3,4) after the administration of a single bolus of ketamine-xylazine. During the ensuing deep phase of anesthesia ($\sim$45 min), the amplitude of δ-waves is strongly pronounced. As the subsequent light phase of anesthesia ($\sim$25 min) is entered, the δ-waves disappear and the amplitude of θ-waves increases. We use the phase dynamics approach to propose a model that incorporates regional ensembles of neurons that are connected both among and between themselves.

Further, we investigate the role played by the neuronal ensembles in temporal coding during deep and light anesthesia from the model results. Neuronal synchrony is often associated with an oscillatory pattern of signals (oscillation-based synchrony). The frequencies of such signals generally cover a broad range and, more importantly, exhibit a marked state dependence. In other words, synchrony and temporal coding of information in selective frequency bands are two different sides of the same coin. We use this idea and establish the link between the conditions under which temporal coding is believed to occur (synchrony) and the level of arousal of the brain.

Physiological background

During periods of slow wave sleep/anesthesia, widespread synchronized oscillations occur throughout the thalamus and the cortex. The slow oscillations ($<$1 Hz) that occur during natural sleep and ketamine-xylazine anesthesia are an emergent network property of neocortical neurons. Those involved are the thalamocortical relay (TC) and thalamic reticular ensemble (RE) neurons (5). The clock-like δ (1–4 Hz) are produced in the thalamus and are strongly synchronized by the RE and the thalamocortical volleys (6). A small proportion of the TC neurons also displays slow and δ-oscillations (5). Thus the high-amplitude, low-frequency δ- and slow oscillations are found to be associated with highly coherent activities of the cortical, RE, and TC neurons. The dynamics of δ- and θ-waves can therefore be represented by interacting ensembles of neuronal oscillators.

The physiological circuitry is as shown in Fig. 1 (*left*) (7). The pyramidal (PY) neurons of the cerebral cortex are connected among themselves (excitatory) by the interneurons (IN), which also form components of the cortical ensemble. The TC neurons receive sensory inputs that are relayed to the

Submitted April 2, 2008, and accepted for publication May 29, 2008.

Address reprint requests to Aneta Stefanovska, Dept. of Physics, Lancaster University, Lancaster LA1 4YB, UK. E-mail: aneta@lancaster.ac.uk.

Editor: Arthur Sherman.

© 2008 by the Biophysical Society
0006-3495/08/09/2722/06 $2.00

doi: 10.1529/biophysj.108.134635

appropriate area of the cortex through ascending thalamocortical fibers (indicated by the *upward arrow*). The RE neurons wrap most of the dorsal and ventral aspects of thalamus (8) and act as a bridge between the TC neurons and the thalamic neurons. The dense axons of the RE neurons innervate the TC neurons (9). The corticothalamic fibers (indicated by the *downward arrow*) also leave collaterals within the RE nucleus and dorsal thalamus. The RE neurons thus form a network that surrounds the thalamus. It receives a copy of nearly all thalamocortical and corticothalamic activity, and projects connections solely to neurons in the TC region (7). In turn, the axons of the TC neurons give rise to collaterals in the RE nucleus while the parent axon passes through the cerebral cortex (10).

THE MODEL

Based on the physiological phenomena that take place during anesthesia, as well as on anatomy, the model system considered is shown schematically in Fig. 1 (*right*). The oscillators in the three ensembles, namely the cortical, the thalamic reticular, and the thalamocortical relay neurons, have different mean natural frequencies and their interactions are characterized by intrapopulation and interpopulation coupling parameters.

Each neuron in the ensembles is considered as an oscillator whose membrane potential is the oscillating variable. The couplings represent the synaptic connections between them. We reduce the system to a phase model, one of the simplest yet accurate models for weakly coupled nonlinear oscillators, with the coupling being introduced through the phases. In doing so, we make use of the fact that there exists a degree of coherence between the membrane potential oscillations and the action potential firings. Although they are not equivalent, the action potentials are triggered at a certain phase of the membrane potential oscillations. This reasoning leads to the following set of equations:

$$\theta_i^{(1)} = \omega_i^{(1)} - \frac{A_c}{N}\sum_{j=1}^{N}\sin(\theta_i^{(1)} - \theta_j^{(1)} + \alpha) - \frac{B_c}{N}\sum_{j=1}^{N}\sin(\theta_i^{(1)} - \theta_j^{(2)} + \alpha) + \eta_i^{(1)},$$

$$\theta_i^{(2)} = \omega_i^{(2)} - \frac{A_{tc}}{N}\sum_{j=1}^{N}\sin(\theta_i^{(2)} - \theta_j^{(2)} + \alpha) - \frac{B_{tc}}{N}\sum_{j=1}^{N}\sin(\theta_i^{(2)} - \theta_j^{(1)} + \alpha) - \frac{C_{tc}}{N}\sum_{j=1}^{N}\sin(\theta_i^{(2)} - \theta_j^{(3)} + \alpha) + \eta_i^{(2)},$$

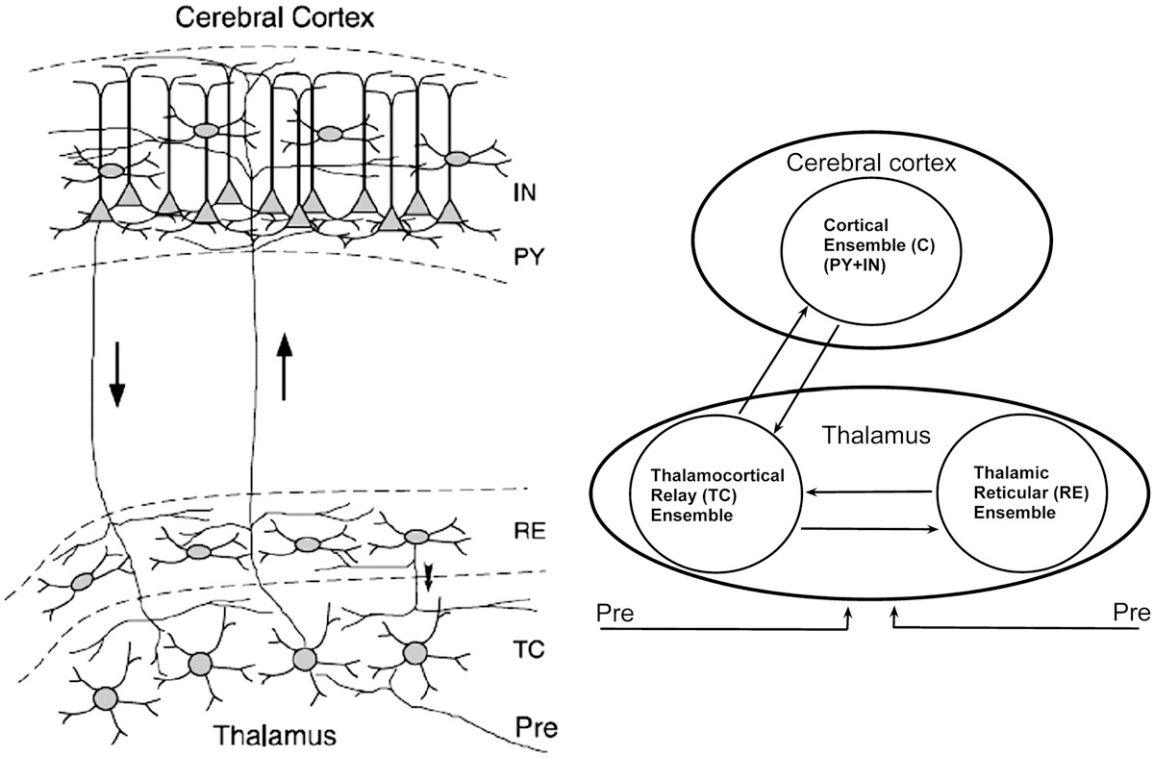

FIGURE 1 (*Left*) Arrangements and connectivity of three groups of cells, namely the TC, RE, and C (composed of the IN and PY cells). ''Pre'' refers to external prethalamic afferent sensory inputs. The upward and downward arrows represent the thalamocortical and corticothalamic fibers, respectively. The figure was reproduced from Destexhe and Sejnowski (7), with permission. (*Right*) Schematic representation of the model. There are three ensembles: cortical neurons (C), thalamocortical relay neurons (TC), and thalamic reticular neurons (RE). They interact both among themselves (represented by the *circle* in each case) and between each other (represented by the *arrows*). The upward and the downward arrows indicate the thalamocortical and corticothalamic connections. External afferent (prethalamic) inputs to the thalamus are denoted as Pre.

$$\theta_i^{(3)} = \omega_i^{(3)} - \frac{A_{re}}{N}\sum_{j=1}^{N}\sin(\theta_i^{(3)} - \theta_j^{(3)} + \alpha) - \frac{B_{re}}{N}\sum_{j=1}^{N}\sin(\theta_i^{(3)} - \theta_j^{(2)} + \alpha) + \eta_i^{(3)}, \quad (1)$$

where $\theta_i^{(1,2,3)}$ are the phases of the ith oscillator in the cortical (C), TC, and RE ensembles, respectively, and N refers to the ensemble sizes. The parameters A_c, A_{tc}, and A_{re} quantify intraensemble couplings within the cortical, thalamocortical, and reticular thalamic ensembles, respectively; B_c corresponds to coupling between the cortical and thalamocortical ensembles; B_{tc} and C_{tc} represent the coupling strengths of the thalamocortical ensemble with the cortical and the thalamic reticular ensembles, respectively; and B_{re} quantifies the coupling between the thalamic reticular and thalamocortical ensembles. The natural oscillator frequencies $\omega_i^{(1,2,3)}$ are assumed to be distributed with central frequencies $\bar{\omega}^{1,2,3}$. The noise terms $\eta_i^{(1,2,3)}$ are added to the model to account for external stimuli coming from the peripherals and other systems in the body, represented schematically as Pre (prethalamic inputs) in Fig. 1. They are independent white Gaussian noises for which $\langle\eta_i^{(1,2,3)}(t)\rangle = 0$ and $\langle\eta_i^{(1,2,3)}(t)\eta_j^{(1,2,3)}(t)\rangle = 2D_{(1,2,3)}\delta(t-t')\delta_{ij}$; $D_{(1,2,3)}$ are the noise intensities. For convenience, one can define complex-valued, mean-field, order parameters as $r_{(1,2,3)}e^{i\psi_{(1,2,3)}} = 1/N\sum_{j=1}^{N}e^{i\theta_j^{(1,2,3)}}$. Here $\psi_{1,2,3}(t)$ are the average phases of the oscillators in the respective ensembles and $r_{1,2,3}(t)$ are measures of the coherence of the oscillator ensembles, which vary from 0 to 1. With these definitions, Eqs. 1 become

$$\begin{aligned}
\theta_i^{(1)} &= \omega_i^{(1)} - r_1A_c\sin(\theta_i^{(1)} - \psi_1 + \alpha) - r_2B_c\sin(\theta_i^{(1)} - \psi_2 + \alpha) + \eta_i^{(1)},\\
\theta_i^{(2)} &= \omega_i^{(2)} - r_2A_{tc}\sin(\theta_i^{(2)} - \psi_2 + \alpha) - r_1B_{tc}\sin(\theta_i^{(2)} - \psi_1 + \alpha) - r_3C_{tc}\sin(\theta_i^{(2)} - \psi_3 + \alpha) + \eta_i^{(2)},\\
\theta_i^{(3)} &= \omega_i^{(3)} - r_3A_{re}\sin(\theta_i^{(3)} - \psi_3 + \alpha) - r_2B_{re}\sin(\theta_i^{(3)} - \psi_2 + \alpha) + \eta_i^{(3)}. \quad (2)
\end{aligned}$$

Numerical methods

A fourth-order Runge-Kutta routine is used for the numerical simulation with the initial phases equally distributed within $[0, 2\pi]$. The results are normalized to ''real time'' and the system is simulated for the equivalent of 60 min with $N =$ 10,000. We will refer to synchrony within an ensemble as intraensemble synchrony, and that between ensembles as interensemble synchrony. The amount of intraensemble synchrony is measured by the mean field parameters: $r_{(1,2,3)} = 0$ implies that there is no synchrony in the corresponding ensemble, $r_{(1,2,3)} = 1$ indicates complete synchrony, and $0 < r_{(1,2,3)} < 1$ corresponds to partial synchrony. The greater the value of $r_{(1,2,3)}$, the more oscillators are oscillating in synchrony (11,12). On the other hand, interensemble synchrony occurs when oscillators from two different ensembles entrain to a frequency/phase window. In general, interensemble synchrony can be quantified by a constant difference in the mean phases $\psi_{(1,2,3)}$. However, this measurement will be valid only if both the ensembles are completely locked to each other. For partial synchrony, the difference in the mean phase will be oscillating, showing no synchrony. Hence we identify interensemble synchrony by looking at the time evolution of the ensemble-averaged frequencies. Also, for increasing interensemble coupling parameters, a decrease in $r_{(1,2,3)}$ is a signature of interensemble synchrony (13).

The interensemble and intraensemble coupling parameters are swept in time to mimic the effect of decreasing concentration of anesthetic agent. This corresponds to the ability of anesthetics to affect thalamocortical signaling, as is well recognized from in vivo electrophysiological work on animals (14). The greater the concentration of anesthetic, the weaker is the interaction among the neurons. Passage from the deeper to lighter anesthetic phases corresponds to a decrease in the concentration of the anesthetic agent. As a first-order approximation, we assume this to occur linearly. In the model, therefore, we increase the coupling parameters linearly with time. The starting values are as given in the legend of Fig. 2. We used a step-size of 0.000027 and increased the coupling values linearly with time, the number of iterations totaling 36,000. Hence, at the end of the simulation, each coupling parameter had increased by 0.972 from its starting value. We introduce asymmetry in the model by a phase shift $0 \le \alpha < \pi/2$. For the values of the mean frequencies, we follow Amzica et al. (15,16): $\bar{\omega}^{(1)} = 3$ Hz, $\bar{\omega}^{(2)} = 1.5$ Hz, and $\bar{\omega}^{(3)} = 1$ Hz, with Lorentzian distributions $g(\omega^{(1,2,3)}) = \gamma/\pi(\gamma^2 + (\omega - \bar{\omega}^{(1,2,3)})^2)^{-1}$.

Our choice of values for the mean frequencies reflects the intrinsic properties of the neurons. The cortical neurons are endowed with intrinsic properties that could be reflected in field potential recordings as δ-activities. The frequencies of these faster oscillations evolve around the upper limit of the δ-band (mainly 3–4 Hz) (15–17). The clocklike δ-oscillations (1–4 Hz) are mainly produced in the RE neurons (5). Individual TC neurons are capable of producing Ca^{2+} spikes and associated action potentials at frequencies of 0.5–4 Hz (6).

RESULTS

The time evolution of the mean frequency of each ensemble is plotted in Fig. 2 (*right*). They represent the time evolutions of the ensemble-averaged frequencies; that is, the frequencies are averaged over all the neurons in each ensemble, and the resulting mean value is plotted against time for each ensemble. For comparison, the experimental δ- and θ-frequencies, obtained by wavelet analysis of the EEG signals from anesthetized rats (3), are plotted in Fig.2 (*left*). In the

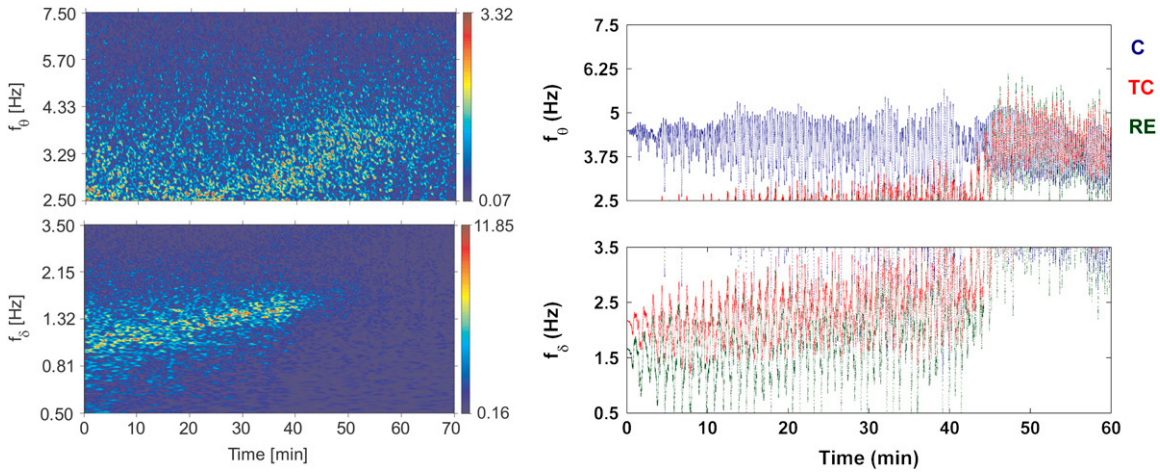

FIGURE 2 (*Left*) Time evolution of the characteristic EEG δ- and θ-frequencies during ketamine-xylazine anesthesia, analyzed by wavelet transform. Reproduced from Musizza et al. (3), with permission. (*Right*) Time evolution of the characteristic δ- and θ-frequencies displayed by three ensembles: C (*blue*), TC (*red*), and RE (*green*), as obtained from the model. The (starting) values of the (coupling) parameters were $A_c = 0.8$, $B_c = 1.2$, $A_{tc} = 0.9$, $B_{tc} = 0.45$, $C_{tc} = 0.9$, $A_{re} = 0.2$, $B_{re} = 0.65$, $\alpha = 0.9$, $D_1 = 0.1$, $D_2 = 0.2$, $D_3 = 0.15$, and $\gamma = 0.4$.

latter experiments, the δ-activity was found initially to be of higher amplitude compared to that of the θ-waves. In particular, during the deep phase of anesthesia (up to ~45 min), there occurs a strong, high amplitude δ-activity that greatly diminishes on entry to the light phase (after ~45 min). The θ-activity runs independently throughout the whole period of anesthesia, but at a much lower amplitude compared to that of the δ-waves. Note the differences in the amplitudes corresponding to the color codes in Fig. 2 (*left*), which makes the θ-activity visible in the top panel.

The model results suggest that it is the TC and RE ensembles that generate the δ-activity during deep anesthesia. This δ is of high amplitude due to the strong synchrony in and between the TC and RE ensembles. Synchrony between the TC and RE ensembles can be easily established even with a smaller value of interensemble coupling, because the frequency difference between them is relatively small. Fig. 3 shows the time evolutions of the mean-field parameters $r_{(1,2,3)}$ of the three ensembles corresponding to the simulated frequencies. During deep anesthesia, the fractions of oscillators that oscillate in synchrony in the TC and RE ensembles are higher than in the C ensemble. This results in a strongly pronounced δ, whereas the amplitude of θ remains low due to a very low number of oscillators oscillating in synchrony in the C ensemble (see Fig. 3).

On the other hand, for the thalamus (TC + RE) to be synchronized with the cortex, a relatively higher value of coupling strength is required. This occurs at ~45 min, at which point the TC and RE frequencies shift to a higher value to join the C ensemble and produce θ-activity. This is the reason for the sudden diminution of the δ and appearance of θ at ~45 min. Of course, the exact time of occurrence depends on the value of the coupling parameter that we choose. As a consequence of the shift (interensemble synchrony), the amount of intraensemble synchrony is reduced in the TC and RE ensembles (J. H. Sheeba, V. K. Chandrasekar, A. Stefanovska, and P. V. E. McClintock, unpublished data) and hence the θ appears as a low-amplitude activity. We thus quantify the amplitudes of the characteristic δ- and θ-activities by the mean-field parameters $r_{(1,2,3)}$, which reveals the amount of synchrony in each ensemble and hence the amplitude of the oscillations. The intraensemble and interensemble synchronization mechanisms discussed here are generic to systems of coupled oscillator ensembles (11,12,18–23, and J. H. Sheeba, V. K. Chandrasekar, A. Stefanovska, and P. V. E. McClintock, unpublished data).

Phase coding and depth of anesthesia

The δ- and θ-phases play significant roles in coding information when the brain is not in an aroused state, characterized by desynchronized EEG. The level with which the phases are synchronized determines the ability to code in-

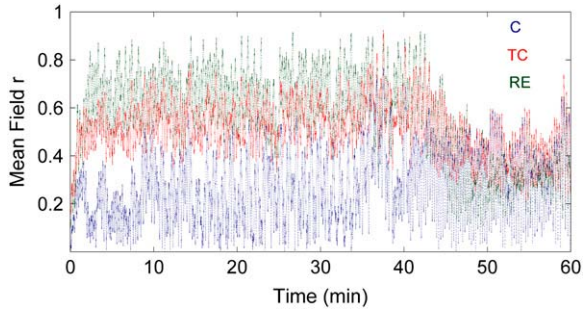

FIGURE 3 Mean-field parameters $r_{(1,2,3)}$ of the three ensembles, plotted as functions of time, corresponding to the frequencies plotted in Fig. 2 (*right*) for the same values of parameters.

formation. However, it is the interensemble synchrony that plays the crucial role in temporal binding (rather than the intraensemble synchrony). Since synchrony is supposed to enhance the significance of responses of the neurons (2), it is obvious that synchronized discharges will have a stronger impact than temporally disorganized ones (24). Thus the θ-phase is found to play a crucial role in inhibiting information by being poorly synchronized in the cortex. More importantly, though, the cortex and the thalamus are not in synchrony with each other (see Fig. 3). Due to this, binding of information cannot be achieved, which is why consciousness and cognition are absent during the deep phase of anesthesia. The strong δ-waves keep the cortex and the thalamus out of phase with each other during deep anesthesia. As the anesthesia lightens, however, the thalamus enters into synchrony with the cortex. We postulate that this corresponds to the onset of awareness when information starts to be coded due to the emergence of interensemble synchrony, characterized by the θ-wave (see Figs. 2 and 3).

DISCUSSION

The model results indicate that the δ- and the θ-activities observed experimentally are separate in terms of their generation and frequency. The δ- and θ-activities are found to occur mainly in 0.5–3.5 Hz and 3.5–7.5 Hz bands in agreement with recent observations (3) and earlier reports (15,16). The dramatic diminution of the δ-amplitude and the simultaneous appearance of θ-activity characterize the transition from deep to light anesthesia.

In the experiment (3), the amplitudes of the δ- and θ-waves differed by more than a factor of 10. To reveal θ (which otherwise would have been lost in the noise level of δ), two separate figures were therefore plotted with different amplitude scales. Our model results suggest that θ-activity is present during both deep and light anesthesia. However, during deep anesthesia, the δ-activity is highly synchronized, whereas θ-activity is poorly synchronized (see Fig. 3). The effect on their relative amplitudes is that the θ-activity cannot be seen during the deep anesthesia in the experiment, consistent with the observations, despite its presence as revealed by the model.

Although varying the coupling parameters to mimic the effect of decreasing concentration of the anesthetic agent helps us to understand and compare the model results with reality, it introduces oscillations in the frequencies. As is evident from Fig. 2, the mean frequencies of each of the ensembles undergo noisy oscillations, while remaining within the δ/θ-bands. The effect of varying coupling parameters affects the frequencies directly because the model equations are for the oscillator phases and the frequencies are calculated from the phases themselves. Likewise, the oscillations seen in the order parameters (Fig. 3) are introduced mainly by the change in interensemble coupling parameters.

Since the model considers only the phases, and not the amplitudes, we are unable to make a direct comparison with the experimental results. However, we make use of the theory of synchronization to quantify the amplitude in terms of the amount of synchrony in each of the ensembles. That is, the more the synchrony, the more oscillators are oscillating in phase with each other, and hence the higher the corresponding oscillation amplitude. On the other hand, the model does offer the advantage that we are able to identify those neuronal groups that are responsible for the generation of δ- and θ-activity during anesthesia.

Although we do not challenge the importance of the microscopic details underlying general anesthesia and the Hodgkin-Huxley formalisms (25), the model results support the hypothesis that consideration of macroscopic dynamics with asymmetry is important. We therefore suggest that models of similar kinds can be used to explain experimental observations, not only in anesthesia, as here, but also in other cognitive and behavioral states that involve huge numbers of neurons functioning in groups. Detailed work has been done in the field of neuronal mass modeling, and a wide range of EEG generative models has been proposed (26–32). Our model is capable of generating the wide range of EEG oscillatory behaviors reported earlier (33–37). Our findings identify the link between neuronal synchrony and temporal coding, especially in terms of interensemble synchrony. An additional advantage of the model is that it yields insight into the synchronization mechanisms underlying the δ- and θ-waves.

CONCLUSION

In summary, we have introduced a model involving asymmetrically interacting ensembles of C, TC, and RE neurons to understand the mechanisms underlying the generation of δ- and θ-waves during anesthesia. The model results are compared with those from experiments (3). The TC and RE ensembles were found to be responsible for the generation of high amplitude δ-waves during deep anesthesia. The C ensemble is engaged with the θ-activity. The transition from deep to light anesthesia is found to be marked by a frequency shift in the TC and RE ensembles, caused by the increase in the coupling strengths. Also, the θ-activity is found not to be as strongly synchronized as the δ-activity. The similarities and differences between the model results and the experimental results were discussed. Furthermore, the model illuminates the phenomenon of temporal coding of information, in particular by the δ- and θ-frequencies. It reveals the role played by the neuronal phases in inhibiting information during deep anesthesia and coding the sensory information during light anesthesia. Although our main motivation for introducing the model was to understand the mechanisms giving rise to the generation of δ- and θ-waves during ketamine-xylazine anesthesia in rats (3,4), it can also be used to elucidate the mechanisms involved in the generation of brain waves for other anesthetics and also during slow wave sleep. The results derived from the model

will have implications for the understanding of functional magnetic resonance imaging (fMRI) and magnetoencelaphographic (MEG) dynamics.

The study was supported by the European Commission FP6 NEST-Pathfinder project BRACCIA and in part by the Slovenian Research Agency.

REFERENCES

1. Del Negro, C. A., C. G. Wilson, R. J. Butera, H. Rigatto, and J. C. Smith. 1999. Periodicity, mixed-mode oscillations, and quasiperiodicity in a rhythm-generating neural network. *Biophys. J.* 24:206–214.
2. Singer, W. 1999. Neuronal synchrony: a versatile code for the definition of relations? *Neuron.* 24:49–65.
3. Musizza, B., A. Stefanovska, P. V. E. McClintock, M. Palus, J. Petrovcic, S. Ribaric, and F. F. Bajrovic. 2007. Interactions between cardiac, respiratory and EEG-delta oscillations in rats during anaesthesia. *J. Physiol.* 580:315–326.
4. Stefanovska, A., H. Haken, P. V. E. McClintock, M. Hoic, F. Bajrovic, and S. Ribaric. 2000. Reversible transitions between synchronization states of the cardiorespiratory system. *Phys. Rev. Lett.* 85:4831–4834.
5. Contreras, D., and M. Steriade. 1997. Synchronization of low-frequency rhythms in corticothalamic networks. *Neuroscience.* 76:11–24.
6. Bal, T., and D. A. McCormick. 1996. What stops synchronized thalamocortical oscillations? *Neuron.* 17:297–308.
7. Destexhe, A., and T. J. Sejnowski. 2003. Interactions between membrane conductances underlying thalamocortical slow-wave oscillations. *Physiol. Rev.* 83:1401–1453.
8. Jones, E. G. 1985. The Thalamus. Plenum, New York.
9. Cox, C. L., J. R. Huguenard, and D. A. Prince. 1996. Heterogeneous axonal arborizations of rat thalamic reticular neurons in the ventrobasal nucleus. *J. Comp. Neurol.* 366:416–430.
10. Harris, R. M. 1987. Axon collaterals in the thalamic reticular nucleus from thalamocortical neurons of the rat ventrobasal thalamus. *J. Comp. Neurol.* 258:397–406.
11. Kuramoto, Y. 1984. Chemical Oscillations, Waves, and Turbulence. Springer-Verlag, Berlin.
12. Pikovsky, A., M. Rosenblum, and J. Kurths. 2001. Synchronization—A Universal Concept in Nonlinear Sciences. Cambridge University Press, Cambridge, UK.
13. J. H. Sheeba, V. K. Chandrasekar, A. Stefanovska, and P. V. E. McClintock. 2008. Routes to synchrony between asymmetrically interacting oscillator ensembles. *Phys. Rev. E.* 78:1(R).
14. Alkire, M. T., R. J. Haier, and J. H. Fallon. 2000. Toward a unified theory of narcosis: brain imaging evidence for a thalamocortical switch as the neurophysiologic basis of anesthetic-induced unconsciousness. *Conscious. Cogn.* 9:370–386.
15. Amzica, F. 2002. In vivo electrophysiological evidences for cortical neuron-glia interactions during slow (<1 Hz) and paroxysmal sleep. *J. Physiol. (Paris).* 96:209–219.
16. Amzica, F., and M. Steriade. 1998. Electrophysiological correlates of sleep δ waves. *Electroencephalogr. Clin. Neurophysiol.* 107:69–83.
17. Steriade, M. 2006. Grouping of brain rhythms in corticothalamic systems. *Neuroscience.* 137:1087–1106.
18. Winfree, A. T. 1980. The Geometry of Biological Time. Springer-Verlag, New York.
19. Okuda, K., and Y. Kuramoto. 1991. Mutual entrainment between populations of coupled oscillators. *Prog. Theor. Phys.* 86:1159–1176.
20. Strogatz, S. H. 2000. From Kuramoto to Crawford: exploring the onset of synchronization in populations of coupled oscillators. *Physica D.* 143:1–20.
21. Montbrio, E., J. Kurths, and B. Blasius. 2004. Synchronization of two interacting populations of oscillators. *Phys. Rev. E.* 70:056125.
22. Daido, H., and K. Nakanishi. 2006. Diffusion-induced inhomogeneity in globally coupled oscillators: Swing-by mechanism. *Phys. Rev. Lett.* 96:054101.
23. Kiss, I. Z., M. Quigg, S. H. C. Chun, H. Kori, and J. L. Hudson. 2008. Characterization of synchronization in interacting groups of oscillators: application to seizures. *Biophys. J.* 94:1121–1130.
24. Alonso, J. M., W. M. Usrey, and R. C. Reid. 1996. Precisely correlated firing in cells of the lateral geniculate nucleus. *Nature.* 383:815–819.
25. Hodgkin, A. L., A. F. Huxley, and B. Katz. 1949. Ionic currents underlying activity in the giant axon of the squid. *Arch. Sci. Physiol. (Paris).* 3:129–150.
26. Wilson, H. R., and J. D. Cowan. 1972. Excitatory and inhibitory interactions in localized populations of model neurons. *Biophys. J.* 12:1–24.
27. Nunez, P. 1974. The brain wave equation: a model for the EEG. *Math. Biosci.* 21:279–297.
28. Lopes da Silva, F. H., A. van Rotterdam, P. Barts, E. van Heusden, and W. Burr. 1976. Models of neuronal populations: the basic mechanisms of rhythmicity. *Prog. Brain Res.* 45:281–308.
29. Freeman, W. J. 1978. Models of the dynamics of neural populations. *Electroencephalogr. Clin. Neurophysiol. Suppl.* 34:9–18.
30. Jansen, B. H., and V. G. Rit. 1995. Electroencephalogram and visual evoked potential generation in a mathematical model of coupled cortical columns. *Biol. Cybern.* 73:357–366.
31. Valdes, P. A., J. C. Jimenez, J. Riera, R. Biscay, and T. Ozaki. 1999. Nonlinear EEG analysis based on a neural mass model. *Biol. Cybern.* 81:415–424.
32. David, O., and K. J. Friston. 2003. A neural mass model for MEG/EEG: coupling and neuronal dynamics. *Neuroimage.* 20:1743–1755.
33. Jirsa, V. K., and H. Haken. 1996. Field theory of electromagnetic brain activity. *Phys. Rev. Lett.* 77:960–963.
34. Wright, J. J., P. A. Robinson, C. J. Rennie, E. Gordon, P. D. Bourke, C. L. Chapman, N. Hawthorn, G. J. Lees, and D. Alexander. 2001. Toward an integrated continuum model of cerebral dynamics: the cerebral rhythms, synchronous oscillation and cortical stability. *Biosystems.* 63:71–88.
35. Wright, J. J., C. J. Rennie, G. J. Lees, P. A. Robinson, P. D. Bourke, C. L. Chapman, E. Gordon, and D. L. Rowe. 2003. Simulated electrocortical activity at microscopic, mesoscopic, and global scales. *Neuropsychopharmacology.* 28(Suppl. 1):S80–S93.
36. Rennie, C. J., P. A. Robinson, and J. J. Wright. 2002. Unified neurophysical model of EEG spectra and evoked potentials. *Biol. Cybern.* 86:457–471.
37. Robinson, P. A., C. J. Rennie, D. L. Rowe, S. C. O'Connor, J. J. Wright, E. Gordon, and R. W. Whitehouse. 2003. Neurophysical modeling of brain dynamics. *Neuropsychopharmacology.* 28(Suppl. 1): S74–S79.